

# New Measurement of the $2S$ Hyperfine Interval in Atomic Hydrogen

N. Kolachevsky,<sup>\*</sup> A. Matveev,<sup>\*</sup> J. Alnis, C.G. Parthey, S.G. Karshenboim,<sup>†</sup> and T.W. Hänsch<sup>‡</sup>

*Max-Planck-Institut für Quantenoptik, 85748 Garching, Germany*

(Dated: May 29, 2019)

An optical measurement of the  $2S$  hyperfine interval in atomic hydrogen using two-photon spectroscopy of the  $1S$ - $2S$  transition gives a value of  $177\,556\,834.3(6.7)$  Hz. The uncertainty is 2.4 times less than achieved by our group in 2003 and more than 4 times less than for any independent radio-frequency measurement. The specific combination of the  $1S$  and  $2S$  hyperfine intervals predicted by QED theory  $D_{21} = 48\,953(3)$  Hz is in perfect agreement with the value  $48\,923(54)$  obtained from this experiment.

PACS numbers: 12.20.Fv, 32.10.Fn, 32.30.Jc, 42.62.Fi

Precision measurements of frequency intervals in simple atomic systems and predictions by quantum-electrodynamics theory (QED) supply essential data for determination of fundamental constants (e.g. [1, 2]). These measurements also enable sensitive tests of the theory ensuring high confidence in its calculations. One type of the tests is based on the determination of the hyperfine splitting (HFS) in hydrogen-like systems.

In hadronic atoms the sensitivity of the HFS-based tests is restricted by an insufficient knowledge of the charge and magnetic moment distribution in the nucleus [3]. This is not the case for exotic leptonic systems like muonium [4] and positronium [5] where the sensitivity reaches 100 ppb. The problem with hadronic systems can be lifted up by construction of the specific difference of the  $2S$  and  $1S$  HFS frequencies  $D_{21} = 8f_{\text{HFS}}(2S) - f_{\text{HFS}}(1S)$  for which the nuclear size effects significantly cancel out [6]. In this case the sensitivity of QED tests is mostly restricted by the experimental uncertainty of  $f_{\text{HFS}}(2S)$ .

The  $2S$  HFS frequency is precisely measured in H, D, and  $\text{He}^+$  which allows accurate determination of the  $D_{21}$  difference [8]. The lowest  $D_{21}$  relative uncertainty of 10 ppb (normalized by the Fermi energy) is reached in the  $\text{He}^+$  ion [9, 10], while for H and D the uncertainty is about 100 ppb. The higher accuracy for  $\text{He}^+$  is due to its higher Fermi energy and the possibility to use ion trapping.

In 2003 we implemented an optical method for measuring the  $2S$  HFS frequency in atomic hydrogen by two-photon spectroscopy of the  $1S$ - $2S$  transition on a cold atomic beam [7]. It gave a result of  $177\,556\,860(16)$  Hz improving the previous values of  $177\,556\,860(50)$  Hz [11] and  $177\,556\,785(29)$  Hz [12] measured by radio-frequency spectroscopy. The  $D_{21}$  values deduced from the two most recent measurements of  $48.53(23)$  kHz [12] and  $49.12(13)$  kHz [7] show a discrepancy at the  $2\sigma$  level (with  $\sigma$  being the standard deviation) from the theoretical prediction of  $D_{21}^{\text{theor}} = 48.953(3)$  kHz [6].

In this work we have re-measured  $f_{\text{HFS}}(2S)$  in H using the optical method described in details in [7]. The method relies on the high stability of an optical refer-

ence cavity which allows to accurately measure the frequency difference between two two-photon transitions  $1S(F=0) \rightarrow 2S(F=0)$  (the *singlet*) and  $1S(F=1) \rightarrow 2S(F=1)$  (the *triplet*) recorded sequentially in time. At a nearly zero magnetic field the equality  $f_{\text{HFS}}(2S) = f_{\text{HFS}}(1S) + f_{\text{triplet}} - f_{\text{singlet}}$  is valid, where  $f_{\text{HFS}}(1S) = 1420\,405\,751.768(1)$  Hz [13].

In the new measurement we use a new ultra-stable optical frequency reference [14] as the most critical improvement compared to [7]. From the theoretical side, a re-analysis of the  $2S$  HFS frequency pressure shift shows that its contribution (14 Hz) to the total error budget of the 2003 measurement (16 Hz) was overestimated and is in fact negligible at our experimental conditions.

To measure  $f_{\text{HFS}}(2S)$  we sequentially excite the *singlet* and the *triplet* transitions by the second harmonic of a 486 nm dye laser [15] locked to the Ultra-Low Expansion glass (ULE) reference cavity 1 in horizontal configuration. The stabilized dye laser has a line width of 60 Hz and a frequency drift of about 1 Hz/s. The Allan deviation of the dye laser frequency corrected for the linear drift equals  $5 \times 10^{-14}$  for  $10^3$  s.

To tune the dye laser frequency between two hyperfine transitions, a double pass acousto-optic modulator (AOM) is installed between cavity 1 and the laser (Fig.1). The required frequency detuning of 310 MHz is too high to tune the laser rapidly between the two transitions without taking it out of lock. Thus, it is impossible to use the simultaneous recording scheme applied for the  $2S$  HFS frequency measurement in D [16] and perturbs the 486 nm laser frequency (see further).

We take advantage of the excellent frequency stability of an external cavity diode laser (ECDL) at 972 nm locked to the thermally- and vibrationally compensated ULE cavity 2 described in details in [14]. The cavity's temperature is stabilized at the zero expansion temperature such that the influence of external temperature fluctuations are strongly suppressed. The frequency drift mostly caused by the ULE aging is nearly linear with a slope of approx. +50 mHz/s. The ECDL possesses a line width of 0.5 Hz and a frequency stability of  $4 \times 10^{-15}$  in  $10^3$  s (with the linear drift corrected).

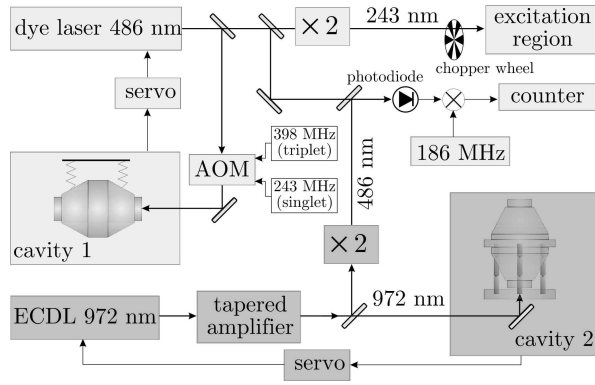


FIG. 1: Laser part of the experiment. The dye laser locked to the ULE cavity 1 in horizontal configuration serves for spectroscopy of the  $1S$ - $2S$  transition in H in the excitation region. To switch between the *singlet* and the *triplet* transitions the double-pass AOM frequency is changed. The 972 nm ECDL is continuously locked to the ULE cavity 2 in vertical configuration and serves as an optical frequency reference. The beat note frequencies of 32 MHz (*triplet*) and 29 MHz (*singlet*) are recorded by the counter simultaneously with the  $1S$ - $2S$  data.

The ECDL is continuously locked to cavity 2 during the whole day of measurement. Its frequency is monitored by a fiber frequency comb referenced to an active H-maser. The optical frequency data are only used to ensure correct and stable operation of the ECDL.

The beatnote frequency between the dye laser and the second harmonic of the ECDL is measured as shown in Fig.1. A local oscillator at 186 MHz is used to create heterodyne beatnote frequencies for both transitions close to 30 MHz which are counted by an HP53131A counter. All synthesizers are referenced to the GPS-disciplined H-maser guaranteeing a fractional frequency uncertainty of  $10^{-14}$ .

The measurement of the beatnote frequency shows that the re-locking of the dye laser causes two effects: First, after re-locking, the dye laser frequency shows an excessive non-linear drift up to a few Hz/s due to transient thermal effects in cavity 1. Second, the re-locking causes abrupt random changes of the laser frequency up to 100 Hz due to insufficient servo loop amplification at low frequencies. Unfortunately, in 2003 we had no possibility to monitor the dye laser frequency during the measurement. The laser instability resulted in excessive data scatter and could be a source of a systematic shift. In the new measurement the instability of the dye laser has basically no influence on the data quality, as the ECDL is never taken out of lock and therefore is free from the described problems.

The second harmonic of the dye laser is coupled to a linear enhancement cavity forming a standing wave for Doppler-free two-photon spectroscopy. Atomic hydrogen produced in a microwave discharge is cooled down

to 4-7 K by a copper nozzle and escapes along the cavity axis. A part of the atoms is excited to the  $2S$  state during their flight in the laser field. The  $2S$  state is quenched in the detection region at a distance of 19.5 cm from the nozzle by an electric field of 10 V/cm (quench field 1). The  $2S$  population is measured by counting the Lyman- $\alpha$  photons. Compensation coils together with  $\mu$ -metal shielding suppress magnetic fields in the interrogation volume. A part of the volume (18 cm) is surrounded by additional magnetic shielding taken from experiment [16] which also plays a role of the beam collimator, and a Faraday cage. This shielding separates the high-vacuum region ( $\lesssim 10^{-7}$  mbar) from the rest of the vacuum chamber ( $\lesssim 10^{-5}$  mbar). All parts of the apparatus surrounding the beam are coated by graphite to suppress stray electric fields.

Compared to [7] we use a cryogenic nozzle with bigger diameter of 2.2 mm which allows to record H lines up to 1 hour without melting the  $H_2$  film from it. The film improves the  $2S$  count rate, but at some thickness it shuts the 243 nm laser beam off. After melting, we wait until the count rate stabilizes before we start the measurement again. An additional electrode is installed close to the nozzle to optionally quench the  $2S$  atoms excited in the nozzle region (quench field 2).

We use time-of flight detection to study different velocity groups in the cold atomic beam. The excitation light is chopped at 160 Hz, and a multi-channel scaler records counts falling into 12 time bins starting at  $\tau = 10, 210, \dots, 2210 \mu s$  and finishing at 3 ms after the 243 nm light is closed by a chopper.

The UV power in the enhancement cavity is monitored by a calibrated photodiode installed after the output coupler. To prevent beam-pointing effects we use an integrating sphere ensuring high reproducibility of the measurement. The power of the 243 nm radiation in the enhancement cavity is maintained nearly constant over the whole day of measurement at the level of 300 mW per direction. To take into account the power fluctuations we correct the measured frequencies by the AC Stark shift which is evaluated by a Monte-Carlo code [17]. For  $\tau = 810 \mu s$  the AC Stark shift correction equals 1.3(1) Hz per 1 mW of 243 nm power per direction.

The measurement sequence is the same described in [7]: Groups of 2-4 *singlet* or *triplet*  $1S$ - $2S$  spectra are recorded one after another, the time  $t$  and the AOM frequency corresponding to each line center are defined by a fit. We use either a Lorentzian fit or an unsymmetrical line shape obtained by averaging all superimposed and amplitude-normalized experimental line shapes for each  $\tau$  (hereafter referred to as “averaged line fit”). The *singlet* and *triplet* lines are fitted by the averaged line fit for the given  $\tau$  using 3 parameters: the amplitude  $A$ , the frequency offset  $f_0$  and the background. The difference  $f_{\text{triplet}} - f_{\text{singlet}}$  is obtained from a double linear fit of 4 neighboring groups of corresponding values  $f_0(t)$  after the correction for the

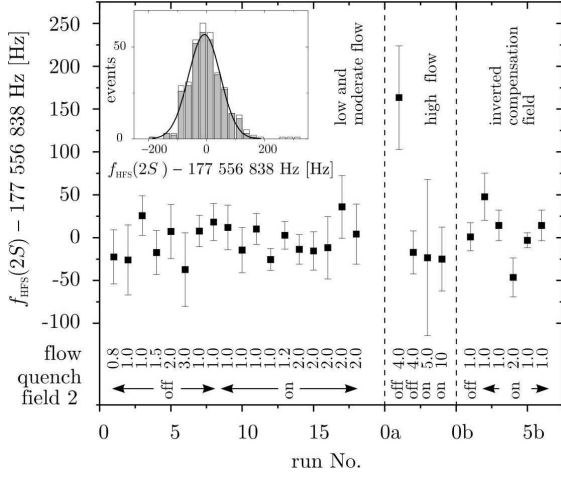


FIG. 2:  $2S$  HFS frequency in H evaluated for  $\tau = 810 \mu\text{s}$  using the averaged line fit. Each data point is the average over one set of measurements at unchanged conditions (particle flow, quench field 2, compensation magnetic field). The histogram shows  $f_{\text{HFS}}(2S)$  data for low and moderate particle flows (gray bars) and all data (white bars) except ones taken at inverted compensation magnetic field.

AC Stark shift. A constant linear drift of the ECDL frequency is assumed during recording of each 4 groups which takes  $10^3$  s. We avoid to use the line shape model with extrapolation to the zero velocity due to its 20 Hz uncertainty [15]. The data of each group are typically used 4 times in the evaluation resulting in the correlation of each 4 neighboring  $f_{\text{HFS}}(2S)$  data points.

During 17 days of measurement in February-April 2008 about 1200  $1S$ - $2S$  hydrogen spectra have been recorded in 28 sets (Fig. 2). Three types of tests were performed: (i) variation of the particle flow coming to the cold nozzle in the range 0.8-10 units (one unit =  $10^{17} \text{ s}^{-1}$ ), (ii) the quench field 2 switched on/off, (iii) the direction of the compensation magnetic field is reversed. Further we consider the most important systematic effects.

*The collisional shift.* In 2003 we set the upper bound for the  $2S$  HFS interval frequency shift as the total shift of the  $2S$  level (8 MHz/mbar, [7]). Now we theoretically analyze the shift which appears only in the third order of perturbation theory if collisions with  $\text{H}(1S)$  are considered [18]. Integration over the discrete spectrum gives a result on the order of 10 Hz/mbar, a similar contribution from the continuum is expected. The intra-beam pressure in the nozzle is  $10^{-4}$  mbar and rapidly decreases in the expanding beam so we can neglect the shift. Proper analysis of collisions with  $\text{H}_2$  molecules is difficult, but since the Wan-der-Vaals interaction does not couple the closely laying  $2S$  and  $2P$  levels, we expect the effect of the same size as for the  $\text{H}(1S)$  partner. Moreover, most of the  $\text{H}_2$  molecules coming to the nozzle from the discharge freeze at its walls. A much stronger effect may be

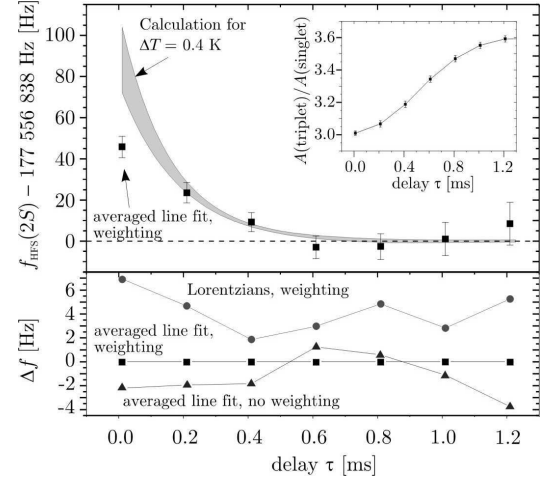


FIG. 3: Top: Averaged experimental  $f_{\text{HFS}}(2S)$  results for different  $\tau$  (squares). Only the left column of the data in Fig. 2 is used for analysis. The gray  $1\sigma$  area shows the expected frequency shift for  $\Delta T = 0.4 \text{ K}$ . Inset: The amplitude ratio of the *triplet* and *singlet* transitions. Bottom: mutual deviation of averaged HFS interval frequencies for different evaluation methods.

induced by the dipole interaction with resonantly photoionized H [10]. But since there are only 10 protons present in the excitation zone at a time the ion collision rate is totally negligible.

We extrapolate the data of Fig. 2 to zero flow separately for each of the time bins. No systematic deviation between the extrapolated and the averaged values is observed. For  $\tau = 810 \mu\text{s}$  the difference equals 1 Hz with uncertainties of 11 Hz and 6 Hz correspondingly. The data taken at higher flows have an excessive scatter due to an instability of the overloaded cryogenic vacuum system (nozzle freezing, fluctuations of the count rate), so we decide to exclude the high pressure data (shifting the final value by  $+0.5\sigma$ ) from the further analysis based on the simple data averaging without adding any systematics.

*Line shape / beam temperature.* We analyze the averaged data from the left column of Fig. 2 for different delays  $\tau$  (Fig. 3, top) which shows a significant increase of the measured  $f_{\text{HFS}}(2S)$  frequency for shorter delays. The analysis of the line shapes indicates that the  $2S(F=0)$  atoms have a higher temperature  $T$  than the  $2S(F=1)$  ones (assuming a Maxwellian distribution). The amplitude ratio of the two hyperfine transitions varies from 3.1 to 3.6 depending on  $\tau$  (see the inset) which means that the fraction of slow *singlet* atoms is less than for the *triplet* ones. In 2003 the effect was observed as well, but the data scatter made an interpretation impossible.

Fitting the *singlet* and *triplet* lines by line shapes simulated for different beam temperatures [17] we find for the difference  $\Delta T = \langle T_{\text{singlet}} \rangle - \langle T_{\text{triplet}} \rangle = 0.4 \text{ K}$  at the

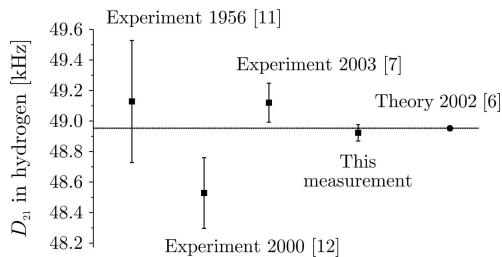


FIG. 4: Experimental and theoretical values for the  $D_{21}$  difference in atomic hydrogen.

average temperature  $\langle T_{\text{singlet}} \rangle = 4.2$  K. The thermalization of hydrogen atoms on the  $\text{H}_2$  film obviously depends on its spin state, but we have no proper explanation of the effect, yet.

We have evaluated the expected shift of  $f_{\text{HFS}}(2S)$  vs.  $T$  for different  $\tau$  by the Monte-Carlo simulations. The dependencies turned out to be nearly linear with the slopes of 220(40) Hz/K ( $10 \mu\text{s}$ ), 68(5) Hz/K ( $210 \mu\text{s}$ ), 17(4) Hz/K ( $410 \mu\text{s}$ ), 5(3) Hz/K ( $610 \mu\text{s}$ ), and 0(2) Hz/K for higher delays (Fig. 3). The uncertainties result from numerical errors and possible jitter of  $\tau$  at a level of  $20 \mu\text{s}$ . As expected, the effect vanishes at higher  $\tau$  since the velocity distribution of the delayed atoms is insensitive to the beam temperature. The optimal compromise between the statistical uncertainty and the effect of different beam temperatures is reached at  $\tau = 810 \mu\text{s}$ .

The influence of the fitting model and data weighting is analyzed in Fig. 3 (bottom). An indication for a model-dependent systematic shift is observed: The Lorentzian fit of strongly asymmetrical spectra for  $\tau = 10 \mu\text{s}$  results in a shift of 7 Hz. On the other hand, the line shape for  $\tau = 810 \mu\text{s}$  is indistinguishable from a Lorentzian, so we expect this effect to reduce to the sub-hertz level. For  $\tau = 810 \mu\text{s}$  we get a 2S HFS interval frequency of 177 556 835.3(6.2) Hz and add 2 Hz uncertainty for line shape/beam temperature shifts.

*The AC Stark shift.* The differential AC Stark shift of the 2S hyperfine components is negligible ( $\sim 1 \mu\text{Hz/mW}$  [7]). Though the difference in *singlet* and *triplet* excitation powers is taken into account for each individual spectrum, the uncertainty of correction itself may cause an error in  $f_{\text{HFS}}(2S)$ . Comparison of the data evaluated with/without correction shows a systematic difference from 2 Hz to 5 Hz depending on the delay  $\tau$ . Assuming an error in the AC Stark shift evaluation of 30 % (including the error in the power measurement), the contribution to the final uncertainty budget is 1.3 Hz.

*The DC Stark shift.* We have no possibility to measure stray electric fields in our apparatus and evaluate its contribution of  $-1(1)$  Hz as in [7]. The influence of the quench fields is tested by the help of Monte-Carlo simulations [17], an effect on the sub-hertz level is expected.

TABLE I: Uncertainty budget for the new 2S HFS frequency measurement in atomic hydrogen.

|                             | Frequency [Hz] | Uncertainty [Hz] |
|-----------------------------|----------------|------------------|
| Averaged interval frequency | 177 556 835.3  | 6.2              |
| Line shape/temperature      | 0              | 2                |
| DC Stark shift              | -1             | 1                |
| AC Stark shift              | 0              | 1.3              |
| Magnetic fields             | 0              | 0.5              |
| final result                | 177 556 834.3  | 6.7              |

*Magnetic fields.* The sensitivity of  $f_{\text{HFS}}(2S)$  to an external magnetic field  $B$  equals  $+9\,600\,B^2 \text{ Hz/G}^2$ . Most of the interaction region (18 cm) is surrounded by a demagnetized shielding with the suppression factor of 300, while zones close to the nozzle and the detector are shielded by a simple  $\mu$ -metal foil suppressing external fields to only 30 mG. In 5 sets of measurements (Fig. 2) the external field is increased to 300 mG by changing of the compensation field direction. The corresponding  $f_{\text{HFS}}(2S)$  differs from the value measured with proper orientation by  $-3(12)$  Hz at  $\tau = 810 \mu\text{s}$ . Comparison of the data sets with quench field 2 switched on and off also shows no significant difference. We estimate the uncertainty resulting from magnetic fields as 0.5 Hz.

Summarizing the uncertainties (Table I) we get the final result of 177 556 834.3(6.7) Hz. The corresponding  $D_{21}$  value is in perfect agreement with the theoretical prediction (Fig. 4). Further improvement could be possible by full automatization of the measurement to accumulate more data. Unfortunately, freezing of the cryogenic nozzle still requires manual interventions.

N.K. acknowledges support from the RSSF and grant MD-887.2008.2, S.K. is supported by DFG #GZ 436 RUS 113/769/0-3 and RFFI #08-02-91969. The authors are grateful to Th. Udem, G. Gabrielse, and M. Herrmann for stimulating discussions.

\* Also at P.N. Lebedev Physical Institute, Moscow, Russia

† Also at D.I. Mendeleev Institute for Metrology, St. Petersburg, Russia

‡ Also at Ludwig-Maximilians-University, Munich, Germany

- [1] F. Biraben, arXiv:0809.2985v1
- [2] M. Hori *et al.*, *Phys. Rev. Lett.* **96**, 243401 (2006)
- [3] M.I. Eides, H. Grotch, and V.A. Shelyuto, *Phys. Rep.* **342**, 63 (2001)
- [4] W. Liu *et al.*, *Phys. Rev. Lett.* **82**, 711 (1999)
- [5] M.W. Ritter, P.O. Egan, V.W. Hughes and K.A. Woodlev *Phys. Rev. A* **30**, 1331 (1984)
- [6] S.G. Karshenboim and V.G. Ivanov, *Phys. Lett. B* **524**, 259 (2002); *Euro. Phys. J. D* **19**, 13 (2002)
- [7] N. Kolachevsky, M. Fischer, S.G. Karshenboim, T.W. Hänsch, *Phys. Rev. Lett.* **92**, 033003 (2004)
- [8] S.G. Karshenboim *et al.*, *Nucl. Phys. B* **162**, 260, (2006)

- [9] H.A. Schüssler *et al.*, *Phys. Rev.* **187**, 5 (1969)
- [10] M.H. Prior and E.C. Wang, *Phys. Rev. A* **16**, 6 (1977)
- [11] J.W. Heberle, H.A. Reich, and P. Kusch, *Phys. Rev.* **101**, 612 (1956)
- [12] N.E. Rothery, E.A. Hessels, *Phys. Rev. A* **61**, 044501 (2000)
- [13] N. Ramsey, *Hyperfine Interactions* **81**, 97 (1993)
- [14] J. Alnis *et al.*, *Phys. Rev. A* **77**, 053809 (2008)
- [15] M. Fischer *et al.*, *Phys. Rev. Lett.* **92**, 230802 (2004)
- [16] N. Kolachevsky, P. Fendel, S.G. Karshenboim, T.W. Hänsch, *Phys. Rev. A* **70**, 063503 (2004)
- [17] N. Kolachevsky *et al.*, *Phys. Rev. A* **74**, 052504 (2006)
- [18] C.M. Dutta, N.C. Dutta, T.P. Das, *Phys. Rev. A* **2**, 30 (1970)